Towards a new method to estimate liquid redistribution coefficients in small fragments of mortar

Toby Cambray[1*], *Valentina* Marincioni[1], and *Hector* Altamirano-Medina [1]

[1]Institute for Environmental Design and Engineering, University College London, United Kingdom

Abstract. Inappropriate replacement mortars in historic buildings often lead to irreparable damage to historic masonry; the influence of the mortar on drying dynamics is crucial to these risks. The chemical and compositional analysis of historic mortar is widely practised for the purposes of formulation of replacement mortars but the compatibility, hygrothermal behaviour and moisture safety mainly depend on the physical properties. The chemistry and composition alone do not give a complete understanding of these functional properties, so physical measurements are necessary. However, it is often the case that only small fragments are available from existing walls due to the thickness of mortar joints, friability of the material and conservation constraints on removing material. While some physical properties lend themselves to measurement with small specimens (pore size distribution, sorption curves), liquid transport is harder to measure accurately for small (<25mm) irregular specimens. A new approach was proposed, combining several established techniques, allowing liquid redistribution to be estimated in such specimens. Specimens were subjected to drying experiments, without the usual constraints to approximate 1D flux (sealing the sides and bottom of a strictly prismatic specimen). The experiment was duplicated in 3D hygrothermal simulation, in which the liquid transport properties were adjusted until the simulation results closely approximated the experimental results. The method was demonstrated on cast cylinders of control materials, and will be developed to cover smaller, irregular pieces in subsequent work.

1 Introduction

Historic mortars have physical properties that protect the masonry units (brick or stone) that they bond from moisture related damage and so practitioners are interested in creating appropriate repair and replacement mortars that will behave in similar ways to the original. Historic lime rich mortars promote drying by virtue of their liquid redistribution properties , [1,2]. These functional properties are primarily mechanical and physical. The majority of analysis of historic mortars is chemical and compositional [3]; while these factors strongly

* Corresponding author: toby.cambray.20@ucl.ac.uk

These proceedings are published with the support of EuLA.

influence the physical and mechanical properties, there are other factors at work such as compaction, water content of the freshly mixed mortar, processing methods of the lime, etc, so it is important to quantify the physical behaviour as well as the chemistry and composition [4].

Some functional properties are easy to measure using small fragments, indeed they are easier and/or faster. These include porosity by mercury porosimetry [1] hygroscopic sorption [4] and pycnometry [5]. Density and capillary saturation can be practically measured using simple methods, needing only sufficiently precise scales/balances, down to a few millimetres fragment size. On the other hand, the particle size of aggregates must be considered, and specimens must be large enough to avoid outlier particles biasing results [6,7].

Liquid transport properties are harder to measure with small specimens. This is because conventional approaches rely on experiments that approximate one-dimensional flows [8–10]. To create these conditions, specimens of several centimetres are cut into prismatic shapes, with sealed sides, and wetted or dried from one face. This is impractical for many mortar specimens, which are limited in size by the thickness of the joints, typically 10 – 15mm in brickwork for example [11]. Due to the size and shapes available, it is often impractical trim such pieces into a true prismatic shape, compounded by the fact that historic mortars are often very fragile and friable, and can contain large-particle aggregates.

An important application for physical analysis is simulation [12] and accurately quantified properties are necessary for proper simulation [13–15]. In the case of historic mortars, the liquid transport is both particularly important, and more difficult to accurately measure. Liquid transport plays a crucial role in the drying process, and the drying behaviour is a crucial mechanism in the protection that historic mortar provides to its stone or brick.

In summary, existing methods for accurately measuring the absorption and drying coefficients of materials rely on sufficiently large and physically robust specimens of regular or prismatic shape and manual handling which introduces experimental error and increases risk of damage to fragile and friable materials. A method that can use small, irregular specimens and that minimises handing would therefore be very useful.

2 Method

A new method was proposed with the intention of enabling small specimens of arbitrary shape to be tested. The method combines several established techniques in a novel way. The method of matching a simulation to an experiment was developed as a practical way to estimate liquid redistribution for commonly used hygrothermal simulation software [13,14]. These parameters are particular to the ‘diffusion analogy’ approach to simulation of liquid transport, but also could be treated as a parameter for e.g. comparison of different mortars or other materials and specification of replacement and repair mortars

A key insight is that existing methods rely on experiments that approximate 1D flux of moisture, to allow representation in 1D simulation. By removing the 1D constraint on the analysis stage, drying experiments on arbitrary 3D shapes can be performed and analysed.

2.1 Preparation and Basic characterisation

Specimens of mortar were cast into cylinders of approximately 48mm diameter, 47mm in height, and allowed to dry and carbonate in lab conditions for 6 months. The mortar recipe based upon mortar from a 1911 red brick building in London. The recipe was proposed by a commercial analysis house, following chemical and compositional tests. The mortar consisted of 1 part NHL2, 1.75 parts grey quartz sand <1.18mm and 0.75 parts charcoal and coal ash <6mm.

Table 1: Basic Characterisation of historic mortar and replacement

Parameter	***Test method***	***Original***	***Replacement***
Density (dry) kg/m^3	Drying at 105°C until dm/dt<0.1% per 24 hr	1357 (5 cuboidal pieces, 20 to 75mm in size)	1684 (5 cast cylinders, 48mm diameter, 47mm high)
Capillary Saturation kg/m^3	Full immersion for 24 hours	344 (5 cuboidal pieces, 20 to 75mm in size)	298 (5 cast cylinders, 48mm diameter, 47mm high)
Total porosity	Helium/N_2 Pycnometry	47% (1 irregular piece approx. 100g)	38% (1 irregular piece approx. 100g)
Absorption coefficient kg/m^2.s$^{0.5}$	Partial immersion as per BS EN 15148 (conventional partial immersion, 1D flux)	0.25 (5 cuboidal pieces, 20 to 75mm in size)	0.019 (5 cast cylinders, 48mm diameter, 47mm high)

These results show that despite being based upon a recipe designed with the input of chemical and compositional analysis, some key physical properties are significantly different. This highlights the importance of establishing the functional parameters of the original material in formulating a replacement.

The sorption isotherm of the replacement mortar, which was used in the experimental stage as a proof of concept, was measured in a Dynamic Vapour Sorption apparatus at a series of humidities up to 90%. These values directly influence the drying simulations that follow, in which the desorption curve was adopted. Values above 90% were linearly interpolated with the capillary saturation moisture content representing 100%. This is a simplification which will introduce error, which will be refined in subsequent work.

Table 2: Sorption Isotherms for replacement mortar

% P/Po	***Change in mass, %***			
	Sorption	***Desorption***	***Sorption***	***Desorption***
0	0.0001	0.0069	0.1616	11.61
10	0.1871	0.1985	315.0	334.3
30	0.2564	0.2800	431.7	471.6
50	0.3094	0.4220	521.0	710.6
70	0.4039	0.5276	680.2	888.6
80	0.5303	0.6282	893.1	1058
85	0.6405	0.7104	1079	1196
87.5	0.7128	0.7572	1200	1275
90	0.8075	0.8075	1360	1360
100 (capillary saturation)	-	-	*1684*	-

2.2 Experimental stage

The experimental stage involves measuring the mass (and hence moisture content) of a specimen continuously or at relatively high frequency, while the initially saturated specimen is dried in conditions of known, stable temperature and humidity and stable air flow.

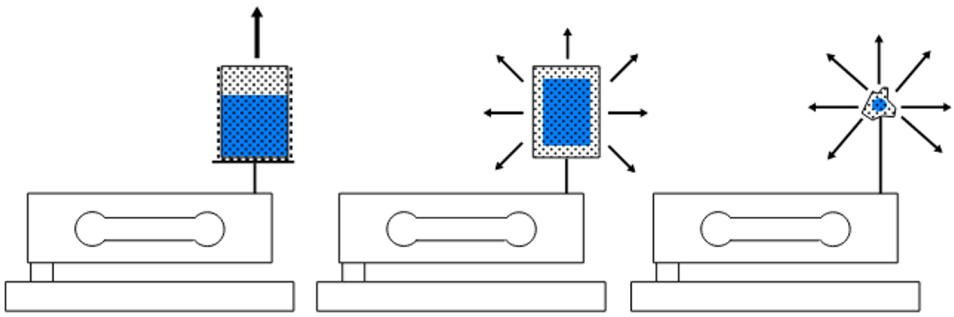

Fig. 1: typical set up of drying experiments, illustrating large, prismatic specimens in 1D and 3D drying, and a small irregular specimen in 3D drying.

Fig. 2: Laminar flow drying apparatus

The vapour permeability also has a strong influence on the drying behaviour. In the context of the proposed method, i.e. performing measurements on small fragments, conventional methods of measuring vapour permeability are impractical, as they require

specimens of around 80mm diameter which are flat and a consistent thickness [16]. Such specimens are subject to the same practical difficulties discussed above.

The set up of the drying experiment is very straightforward, except for the need to control the boundary conditions at the surface of the specimen. Drying can be broadly separated into stage 1 and stage 2, according to the position of the drying front [15,17]. In both stages the vapour pressure is important; experiments should therefore be undertaken in controlled environments to simplify analysis. In the first stage, the vapour pressure gradient at the surface is also important, as this controls the rate of evaporation from the film of water on the surface of the material. The vapour pressure gradient depends on the air flow over the surface. This is not the case in stage 2, because the slower release of moisture into the airstream has a negligible effect on the ambient humidity.

Following basic characterisation, various specimens were saturated by submersion and them placed in a purpose-built, controlled flow wind tunnel, in a climate chamber at constant temperature and humidity of 23°C and 50%RH [8]. The cylindrical specimens were tested twice, once with the bottom and sides sealed to create 1D flux, and secondly without sealing – these experiments are referred to here as 3D. Specimens were dried to equilibrium, with the mass recorded at approximately 2 minute intervals.

2.3 Simulation Stage

Comsol Multiphysics 6.2 was used to perform hygrothermal simulation on the 3D geometry. As described by other authors in 1D [14,18], a hygrothermal simulation of the physical experiment is run in an iterative manner, redistribution coefficients until a good match is established. In this work, the vapour permeability is treated as an additional parameter for optimisation. When a close match has been achieved, the coefficients can be assumed to be representative of the material behaviour for the purposes of hygrothermal simulation.

This paper illustrates the principle using cast cylindrical specimens as a proof of concept, which will be extended to arbitrary shapes in subsequent work. It is planned to capture the geometry of fragments using photogrammetry. The cylindrical geometry can be represented as radially symmetrical, and hence simulated in 2D for the purposes of method development.

Comsol allows material properties and functions to be defined via analytical expressions, or by interpolation from tabulated values. In this paper, the key material functions (sorption isotherm and liquid redistribution coefficient) were set up as tables of values for interpolation, to reflect the input of other software tools, and hence simple transfer of the estimated redistribution values to more commonly used tools. The temperature and humidity were set to the experimental conditions.

The experimental results were processed to give the total moisture content of the specimen, which can be easily compared with a simulation output. Using the sorption isotherm, the equilibrium moisture content at the ambient (experimental) conditions of 23°C and 50% RH was established and compared with the equilibrium mass, volume and dry density of the specimens to ensure a reasonable alignment.

The boundary conditions were represented in simulation as constant at 23°C and 50% RH. The moisture flux is dependent on the vapour pressure gradient, which is represented as a convective transfer coefficient, expressed in Comsol as a moisture transfer coefficient with units of s/m. T

The starting relative humidity of the material in the simulation was then adjusted to align the initial conditions between the simulation and experiment (RH, as opposed to water content, is the input variable for such simulations). The influence of air flow was represented by a surface resistance coefficient, which was adjusted until the slope of the (linear) stage 1 drying matched the experimental behaviour during Stage 1 drying.

Other properties have a direct influence over this behaviour, in particular the moisture storage. Therefore, the sorption isotherm, the dry density and the free water saturation of the material were measured for the material and used as properties for simulation.

The simulated drying behaviour using calibrated redistribution coefficients were compared with the drying behaviour using the simple estimates derived by estimating the suction coefficients from absorption experiments, and dividing by ten [13].

3 Results

3.1 Experimental stage

Figure 3 shows the drying behaviour of two of the 48mm x 47mm cylinders of mortar, exposed to air on all surfaces (3D drying). Stage 1 drying can be clearly identified. The same data are plotted in Figure 4, but against the square root of time. Standard theory predicts a transition period followed by Stage 2 of drying which proceeds in proportion with the square root of time. The start of the transition can be identified as the point when the data diverges from the linear model. Stage 2 begins where the data converges with a trend that reduces proportionally to the square root of time. However, in this case, the transition period is relatively long, and stage 2 does not clearly emerge. The longer time of the transition implies a larger 'fringe' or transition zone between the wet and dry regions. A larger wet-dry fringe makes it more difficult or impossible measure a drying coefficient, especially for small specimens, because the dimension of the fringe exceeds that of the specimen.

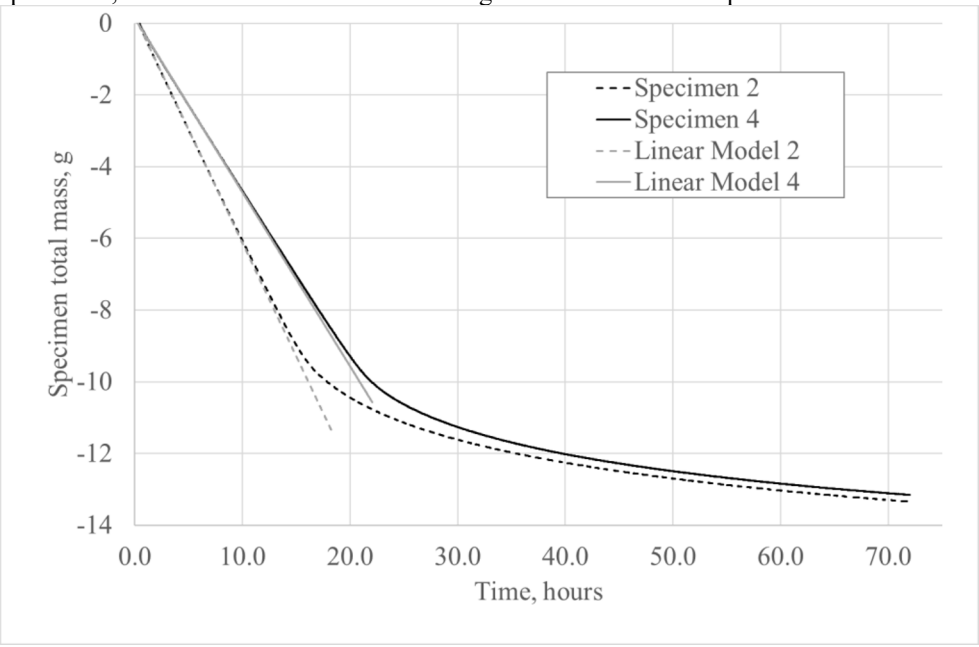

Figure 3: Results of 3D drying test for two specimens

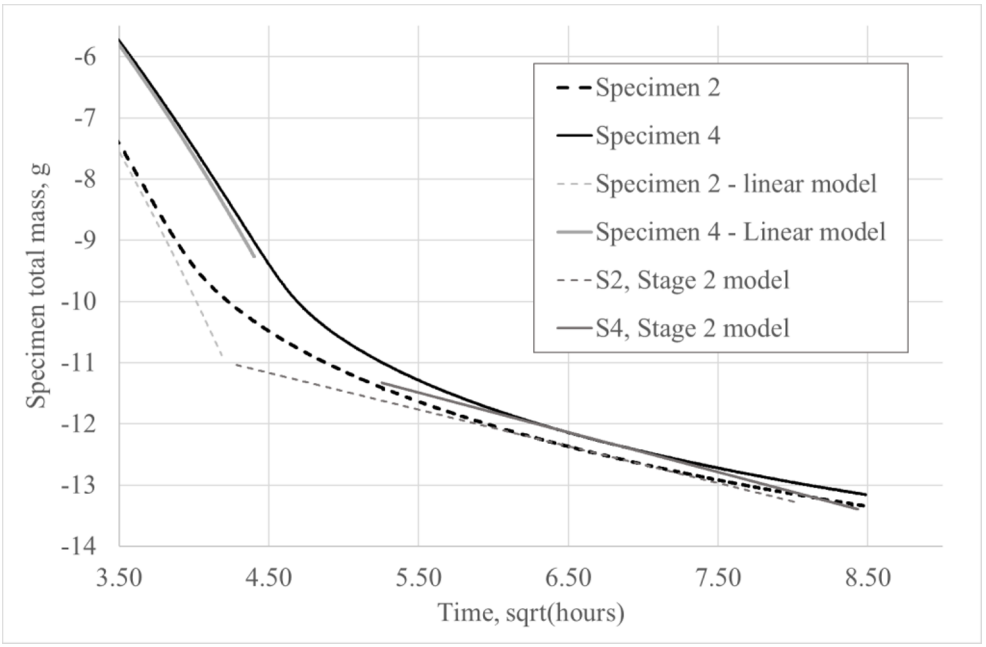

Fig. 4: Results of 3D drying test for two specimens (Boltzmann transform)

For reference, Fig. **5** shows results of a physical experiment on two small (~10mm) and irregular fragments of mortar. Because the surface area to volume ratio is much greater than the 50mm cylinders discussed above, there is only a small amount of moisture lost after stage 1 is completed. This implies that for good results with the proposed method, accuracy of the weighing systems is very important, but the circa 2 minute measurement frequency appears to be sufficient. These results are not considered further in this paper.

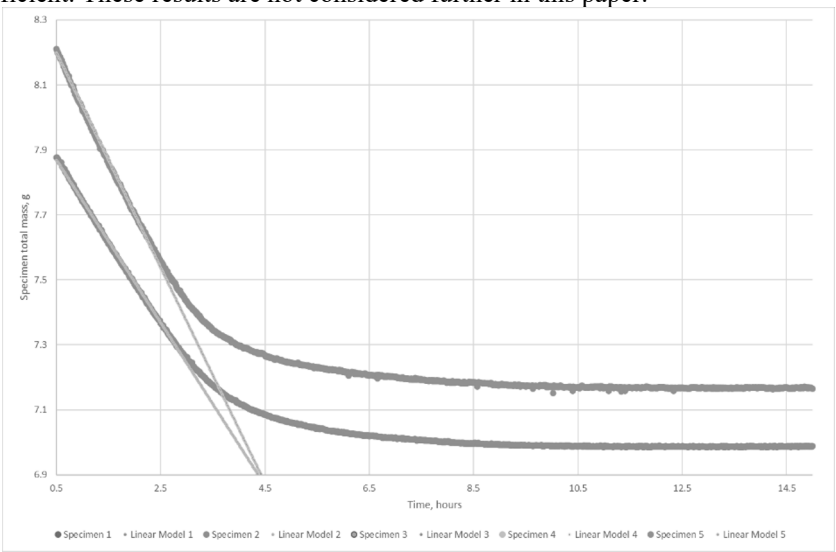

Fig. 5: Example of drying curves for small fragments of mortar

3.2 Simulation stage

Figure 6 shows the simulated relative humidity profile in the specimen at four time steps. The drying from the exposed top, side and bottom can be observed; the left hand edge represents the axis of the cylinder, hence is adiabatic. These results support the observation that the wet-dry fringe dimension exceeds the specimen dimension.

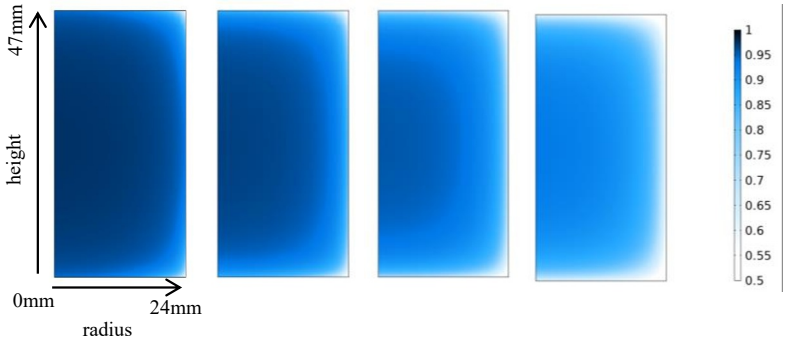

Fig. 6: Humidity profiles in a radial plane of the simulated cylinder at 7, 10, 15 and 25 hours

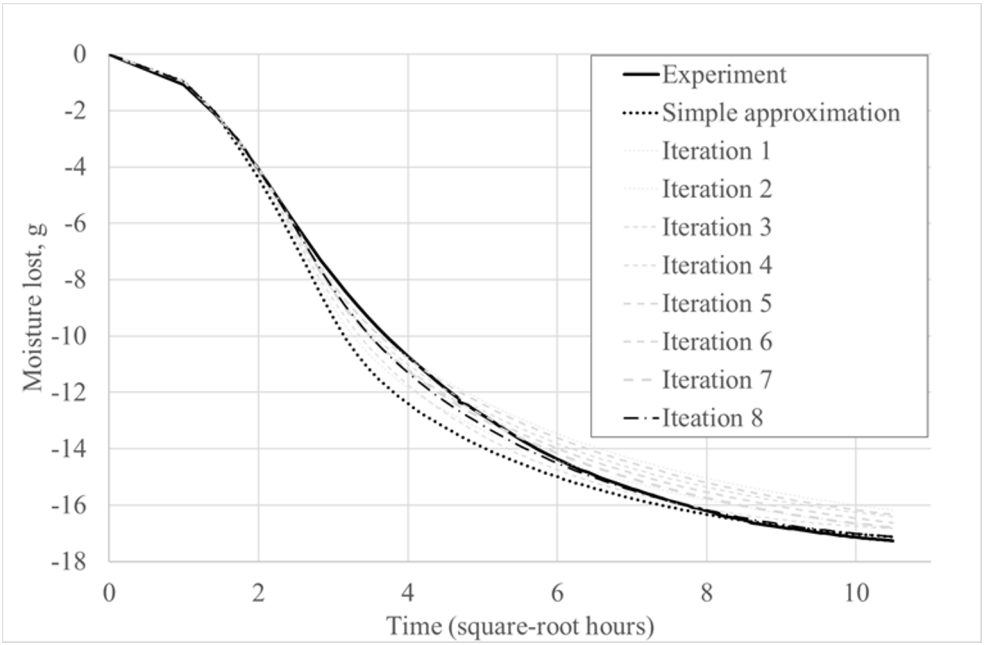

Fig. 7: Results of 8 simulations, illustrating the process of refining the material properties to match the simulation to the experiment

The simulation was refined in an iterative manner, adjusting the vapour permeability and the liquid diffusion coefficients, until the curve predicted by simulation was closely aligned with the experimental observations. **Fig. 7** shows the results of this process, as well as the drying curve predicted by redistribution coefficients estimated by the simple method of

dividing the suction coefficients by 10 [13]. The resulting liquid diffusion properties are as follows:

Table 3: Final calibrated Redistribution coefficients versus simple approximation

Parameter	Value (estimated via 3D simulation)	Value (predicted according to [13])	Difference (ratio)
Vapour resistance factor	10 (-)	-	-
Dww (at capillary saturation)	8.0 x 10^{-9} m^2/s	2.67 x 10^{-7} m^2/s	33
Dww (at W_{80})	2.2 x 10^{-10} m^2/s	1.5 x 10^{-10} m^2/s	1.5

This shows that the simple approximation method overestimates the liquid redistribution by a significant factor, particularly at high moisture content.

4 Discussion and Conclusions

This work shows that the concept of obtaining liquid redistribution coefficients by comparing 1D simulation with 1D drying experiments can be successfully extended into 2D radially symmetrical simulation, compared with 3D drying of a cylinder.

If the technique can be successfully extended to smaller irregular specimens, the characterisation of liquid transport in specimens which were previously too small, irregular and fragile becomes a possibility.

The selected simulation tool appears to be capable of producing the necessary simulations successfully. Moving from an essential 2D (radially symmetrical) simulation to full 3D significantly increases the computational load, but the software allows straight forward adaptation to arbitrary 3D geometry in the future. Almost identical results (within the error of the numerical solutions) were obtained by simulating a full cylinder, defined with a tetrahedral mesh; the solution times increase from around 3 minutes (on an Intel i7, 1.7GHz 16Gb RAM laptop) for the radially symmetric geometry to around 20 minutes for a coarse meshed cylinder.

It was found that the mesh size can influence numerical stability and convergence due to the steepness of the moisture storage function at high relative humidity. This can be mitigated by increasing the mesh (spatial) resolution, but this increases computation demand.

Due to the interaction of these parameters with respect to the drying curve, matching the curves manually is a time consuming process. In future work, this process will be automated using optimisations tools within the software.

The size of the ‘gradient zone’ between the wet and dry zones does not appear to limit the applicability; the zone is large in comparison to even the 50mm cylinders used for the proof of concept.

4.1 Further work

Drying and redistribution have been the focus of this work because these properties are arguably more important in historic mortars, and due to difficulties observed in initial experiments using full immersion absorption. If further work does not overcome these difficulties, liquid suction coefficients could be roughly estimated by multiplying the redistribution coefficients by 10; this would still provide a useful estimate in cases where only small irregular specimens are available.

Next steps include:

- Importing complex, arbitrary geometry of mortar fragments into the software
- Optimise simulation efficiency, especially for arbitrary 3D geometry. Optimisation of mesh size would be a first step; an adaptive mesh strategy may be effective, with smaller mesh elements where the moisture content is changing rapidly, however the time to calculate mesh geometry may outweigh any saving. Adaptive time step control is also likely to aid convergence.
- Validating the 3D cylindrical drying against 1D methods
- Validating the 3D method against full detailed NMR based methods
- Using the method to expand existing databases of functional properties of historic mortars.

References

1. D. Wiggins, Lime Mortar and the Sacrificial Protection of Heritage Masonry, Glasgow Caledonian University, 2015
2. N. Copsey, *Hot Mixed Lime and Traditional Mortars: A Practical Guide to Their Use in Conservation and Repair* (The Crowood Press Ltd, Wiltshire, 2019)
3. G. Bianchini, E. Marrocchino, and C. Vaccaro, Cem. Concr. Res. **34**, 1471 (2004)
4. P. F. G. Banfill, Mater. Struct. **54**, 167 (2021)
5. M. Čáchová, J. Koťátková, D. Koňáková, E. Vejmelková, E. Bartoňková, and R. Černý, Procedia Eng. **151**, 127 (2016)
6. J. Valek and R. Veiga, in (n.d.), p. 365
7. R. Veiga, P. Faria, R. van Hees, M. Stefanidou, P.-N. Maravelaki, I. Papayianni, I. Ioannou, M. Theodoridou, V. Bokan Bosilijkov, B. Bicer-Simsir, C. Tedeschi, and A. Carneiro, Mater. Struct. **56**, 70 (2023)
8. BSI, (2013)
9. BSI, (2016)
10. C. Feng and H. Janssen, Build. Environ. **134**, 21 (2018)
11. A. Arizzi and G. Cultrone, Archaeol. Anthropol. Sci. **13**, 144 (2021)
12. BSI, (n.d.)
13. H. M. Künzel, *Simultaneous Heat and Moisture Transport in Building Components: One- and Two-Dimensional Calculation Using Simple Parameters* (IRB Verlag, Stuttgart, 1995)
14. A. Holm and M. Krus, Restor. Build. Monum. (1998)
15. Scheffler and R. Plagge, in (ASHRAE, 2010), p. 12
16. BSI, (2016)
17. C. Hall and W. D. Hoff, *Water Transport in Brick, Stone, and Concrete*, 2nd ed (Spon Press, London ; New York, 2012)
18. M. Krus, Moisture Transport and Storage Coefficients of Porous Mineral Building Materials : Theoretical Principles and New Test Methods, 1996